Results in Physics 14 (2019) 102518

Contents lists available at ScienceDirect

Results in Physics

journal homepage: www.elsevier.com/locate/rinp

High mobility and transparent ZTO ETM prepared by RF reactive co-sputtering for perovskite solar cell application

M.A. Islam[a,*], K.S. Rahman[a], H. Misran[a], N. Asim[c], M.S. Hossain[d], M. Akhtaruzzaman[c], N. Amin[a,b,*]

[a] Institute of Sustainable Energy, Universiti Tenaga Nasional (@The National Energy University), Jalan IKRAM-UNITEN, 43000 Kajang, Selangor, Malaysia
[b] INTEGRA, Faculty of Engineering and Built Environment, The National University of Malaysia, 43600 Bangi, Selangor, Malaysia
[c] Solar Energy Research Institute, The National University of Malaysia, 43600 Bangi, Selangor, Malaysia
[d] Department of Electrical and Electronic Engineering, Dhaka University of Engineering and Technology, Dhaka, Bangladesh

ARTICLE INFO

Keywords:
ZTO thin film
Reactive co-sputtering
Mobility
ETM
SCAPS-1D
Perovskite solar cells

ABSTRACT

Thin-films of Zinc Tin Oxide (ZTO) with high charge carrier mobility and superior optical transmittance has been prepared by the rf-reactive co-sputtering technique in argon-oxygen (99:01) ambient. These deposited films have been systematically studied to determine the effect of deposition temperature on film structure, composition, and optoelectronic properties. X-ray diffraction (XRD) spectra indicated that the ZTO films remain amorphous even growth temperature increased to 400 °C. The films deposited at room temperature (RT) and 100 °C were slightly tin-rich found in Energy-dispersive X-ray (EDX) spectroscopy compared to the films deposited over 100 °C. It was found that growth temperature played a crucial role in carrier concentration and mobility of the films and such properties are controlled by the grain boundary scattering over the Sn dopant concentration. The transmittance of the films was found above 85% in the visible range regardless of substrate temperature. The complete perovskite solar cell has been numerically analyzed by employing SCAPS-1D software and the effect of ZTO's optoelectrical properties on cell performance has been revealed.

Introduction

Perovskite materials as light harvesters for new-generation photovoltaic application are currently attracting enormous research interest from both scientific and industrial communities in the past few years due to their high efficiency and potentially low production cost [1,2]. Within just few years, from 2009 to 2018, perovskite-based solar cells (PSCs) have shown exceptional improvement in efficiency from 3.8% to 23.3% [3], owing to the material's intriguing optoelectronic properties such as direct bandgap, high absorption coefficient, high charge carrier mobility and lifetime, long carrier diffusion length in the micrometer range and defect tolerance ability [4–8]. Endowed with these unique properties, perovskites have also drawn much more attention in the development of light emitting diodes, optically pumped lasers [9], photo-detectors (PDs) [10] and thermoelectric devices [11]. The highest efficiency obtained in PSC with the mesoscopic structure which is already higher than the commercially available CdTe and CIGS thin film solar cells, however, the intrinsic instability of perovskite devices owing to moisture, heat, and light illumination, hinders their practical application in ambient conditions [12]. It should be noticed that the device structure including Electron-transport materials (ETMs), which extract photo-generated electrons from perovskite layers and transport them to the cathode, play an important role in PSCs performance, stability and degradation [13]. Therefore, the properties of ETMs that is essential for high-performance and highly stable PSCs has also garnered much attention along with the whole device advancement.

Recently, TiO_2, SnO_2, and ZnO are commonly used in PSCs as an electron transport material (ETM) or buffer material. However, besides their numerous advantages as ETM, low electron mobility, high defect density, and low thermal stability affect the efficiency and stability of PSCs. On the other hand, it has been reported that mobility of Zinc-Tin-Oxide (ZTO) is approximately three orders higher than that of TiO_2 and ZnO buffer layer [14]. Also, Aviles and Wu [15] reported that ZTO has much smaller recombination than that of TiO_2 at the front contact interface of the solar cell. Alternatively, to get an ideal ETM for a solar cell, besides the mobility, optical transmittance is also a key factor to ensure enough amounts of photons harvested by the absorber layer. It has also been reported that ZTO is a much more superior buffer layer

* Corresponding authors at: Institute of Sustainable Energy, Universiti Tenaga Nasional (@The National Energy University), Jalan IKRAM-UNITEN, 43000 Kajang, Selangor, Malaysia.
E-mail addresses: aminul.islam@uniten.edu.my (M.A. Islam), nowshad@uniten.edu.my (N. Amin).

https://doi.org/10.1016/j.rinp.2019.102518
Received 14 May 2019; Received in revised form 14 July 2019; Accepted 14 July 2019
Available online 22 July 2019

than ZnO and TiO_2 in terms of the optical transmittance property [16], thus we believe that ZTO could be an ideal material to substitute TiO_2, SnO_2 and ZnO which are conventionally using as ETM in PSCs.

On the whole, TiO_2 is the most extensively studied ETM in PSCs. It's band alignment with the perovskite absorber layer assuring easy electron injection and hole-blocking from the perovskite absorber to the ETM [17]. In addition, the well controllable morphology of TiO_2 is another attractive feature for using widely as ETM in PSCs. [18]. However, low electron mobility, the high density of trap states, light-induced degradation [19], charge accumulation at the interface and hysteresis behavior in current–voltage properties [20] affects the efficiency and stability that influence for looking alternative ETM. Moreover, SnO_2 shows high stability and high electron mobility [21] and using SnO_2 as ETM increase the stability of PSCs over the TiO_2, however, SnO_2 based PSCs are also suffered from poor electron selectivity [22] and notable hysteresis [23]. Additionally, ZnO as ETM seemed more attractive than TiO_2 and SnO_2 for it's larger electron mobility, low-temperature process and hysteresis-free device performance [24] However, the chemical instability with large basicity (8.7) [25] and thermal instability of the ZnO/perovskite bilayer is still a hindrance for its application in PSCs [26].

Alternatively, ZTO seems most potential ETM in PSCs over the above materials. It has appealing photoelectric properties, such as wide optical bandgap (3.8 eV), relatively low refractive index (2.0), lesser electron effective mass (0.23 m_e), high electron mobility (10–30 $cm^2 V^{-1} s^{-1}$), and a comparatively good band alignment with perovskite absorber layer [27]. Also, it has high chemical stability with respect to the acid/base solution and polar organic solvents, has an influence on the crystallization of the $MAPbI_{3-x}Cl_x$ layer, and has the ability to promote the formation of bilayer perovskite structures with uniform crystallization including bigger grains as large as 2.0 μm [28]. All the above properties are indicating ZTO could be an outstanding ETM for PSCs. Moreover, PSCs using ZTO as the ETM showed negligible electrical hysteresis and high stability [27]. The main shortcoming of ZTO for application in PSCs is the high temperature (> 200 °C) required to crystallize it. However, we believe that this temperature could only hindrance for its application in flexible PSCs although Shin et al. [16] already reported a new method to prepare crystalline ZTO nanoparticle at 90 °C and applied them as an ETM in PSCs fabrication via a simple room-temperature solution process [29]. The device shows a remarkable PCE of 17.7% for inverted planar PSCs, with significant ambient stability, retaining over 90% of its original PCE after being stored under 30 ± 5% relative humidity for 14 d [29]. This work already identified ZTO as a promising candidate as an ETM for efficient PSC applications.

Besides, the potential application of ZTO in various optoelectronic field including in sensitized solar cells [30], organic and polymer solar cells [31] and thin film solar cells [32–35] already signifying its potential in photovoltaic applications which motivates for investigating of its structural, optical and electronic properties for applying in PSCs. It should be noticed that due to the wide variety of applications, ZTO has already been studied much more than other relative thin films. However, the ZTO films prepared by the reactive co-sputtering technique is quite less studied unlike solution process methods although sputtering could be the best deposition technique for ZTO thin films. Particularly, the sputtering technique facilitates precise thickness with a controlled amount of desired elemental composition and impurity in a long range. Since the properties of the resulting ZTO films are sensitive to the growth conditions, and significantly affect the development of high-efficiency optoelectronic devices, thus, improved understanding of the relationship between growth conditions and the film structural evolution, morphological, optical and electrical properties are much more crucial not only for enhancement of all practical applications in different types of solar cells mentioned above but also exploring the new possible technological applications of ZTO films. The primary goal of this work is to expand our understanding of ZTO thin films via the analysis of the relationship between deposition temperature and optoelectrical properties of the sputtered ZTO thin films and to use these properties to develop a model of a complete PSC. The numerical model of PSC has been analyzed by employing SCAPS-1D software and the effect of ZTO's optoelectrical properties on cell performance has been briefly studied.

Methodology

ZTO films of the thickness of around 100 nm were deposited by RF magnetron co-sputtering using the commercial ZnO and SnO_2 target (purity 99.999%) supplied by Plasma Materials, Inc. in Ar (99%) with O_2 (1%) ambient on top of the glass substrate. The employed deposition power was 50 W (for both materials) with the ambient pressure in the range of 8–10 mT, and with baseline pressure of below 1.0×10^{-5} T. The pressure was maintained constant for all the films by flowing 2.0 SCCM of mixed Ar:O_2 (99:1) gas. The schematic of the deposition process is shown in Fig. S1. The films were deposited in different substrate temperature, ranging from room temperature (RT) to 400 °C.

The structural properties and surface morphology of the films were investigated using X-ray diffraction (XRD) spectroscopy, and scanning electron microscopy (SEM). The XRD patterns were taken in the 2θ ranging from 10° to 70° using Cu Ka radiation wavelength of 1.5408 Å using 'BRUKER aXS-D8 Advance Cu-Ka' diffractometer. The SEM analyses of the samples were carried out using 'LEO 1450 Vp', respectively. The carrier density, mobility, and resistivity are measured by the Hall Effect measurement by means of 'ECOPIA 3000'. The optical properties are determined by the UV–vis spectrometry using 'Perkin Elmer Instruments Lambda35'. Also, in the present study, a device simulation using one dimensional Solar Cell Capacitance Simulator (SCAPS-1D) software was employed to investigate the influence of ZTO material properties on device behavior of planner PSCs, aiming to understand its physical mechanism and realizing the performance improvement. The significant impact of ZTO's optoelectrical properties on PSCs was observed.

Results and discussion

The structural properties including material phases and crystallinity of the deposited ZTO films at different substrate temperature are investigated through the XRD as shown in Fig. 1. All the films show amorphous nature regardless of growth temperature. Chiang et al. [36] have also been reported that the ZTO deposited via rf magnetron sputtering in Ar/O_2 (90%/10%) ambient has an amorphous structure rather than a crystalline structure. It has also been reported that the

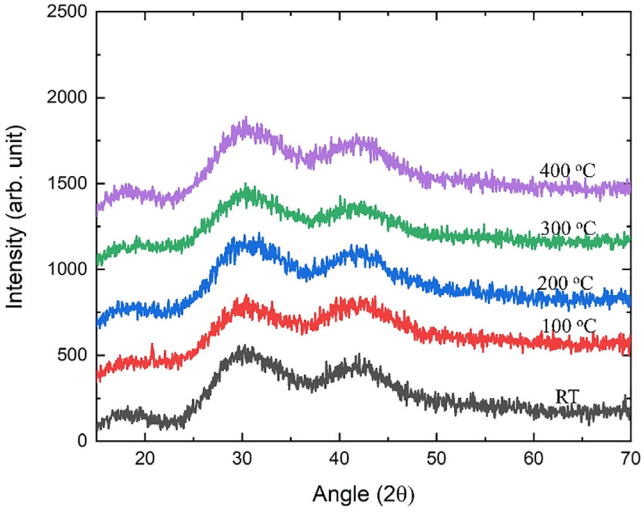

Fig. 1. XRD diffraction patterns of ZTO thin films deposited by reactive co-sputtering at a different substrate temperature (RT to 400 °C).

ZTO films with Zn/Sn ratios close to 2 could become crystalline at higher temperatures (≫500 °C) [37], however, Chidambaram et al. [38] reported that the ZTO films remain amorphous even after annealing to 600 °C. In this study, the films are found amorphous dominant structure because of low growth temperature (highest is 400 °C) which is highly consistent with the reported literature [37,38]. The broad peaks as seen in Fig. 1 indicates that the degradation of the crystalline quality of ZnO and/or SnO_2 films due to the lattice damage produced by the incorporation of Sn atoms to the ZnO lattice or Zn atoms to SnO_2 lattice. Since the ionic radius of Sn is larger than Zn, thus, when their sites are replaced by one another, the lattice deformation started due to compressive strain (when Sn atoms replaced by Zn) and tensile strain (when Zn atoms replaced by Sn), and therefore, the crystalline quality decreases or amorphization in the film gets started. It has also been reported that the integration of additional elements similar to Sn (such as In, Al, or Ga) into the ZnO matrix induces the transformation of crystalline phase into an amorphous phase [39]. The benefits of such amorphous metal oxide thin layer already proven in LED as an electron transport layer which prevent morphologically induced electrical shorts and/or the formation of preferred current channels through the device structure [40].

The dominated amorphous nature in the polycrystalline films found in this study indicates that a large number of grains with various relative positions and orientations leading to lattice misfit and lattice strain. The lattice strains are developed in the films by varying displacement of the atoms as mentioned above with respect to their reference-lattice positions which in turn depends upon the growing conditions of the films [41]. Conversely, the imperfection in a crystal associated with misregistry of the lattice in one part of the crystal with respect to another part of the thin films, which is led by unlike vacancies and interstitial atoms in the crystals. This imperfection in a thin film per unit area known by a term dislocation. From the XRD results, it could be concluded that the films may have a large number of interstitial Sn and/or O atoms and/or interstitial defects that lead to lattice misfit and dislocation in the film structure and embolden the amorphous nature.

Fig. 2 shows the SEM morphology of ZTO films with different substrate temperature. The surface of the film prepared at RT is dense with nanoplatelets, shows very tinny grains, however, other films at a glance shows the nanostructures of spherical shaped grains that are distributed uniformly and covered the entire substrate surface without any pinhole. The compositional analysis was verified by the EDX result as shown in Fig. 2(f), which for only the film prepared at 300 °C of substrate temperature. The spectrum reveals the presence of Zn, Sn and O elements in the deposited films. The variation of elemental compositions in the films is shown in Fig. 4 (next section) in the form of Sn/(Zn + Sn) and O/(Zn + Sn), respectively. The elemental composition of the ZTO thin films confirmed that the atomic concentration of the elemental species is dependent on the growth temperature. Also, the silicon signal appears from the substrate and the trace amounts of C, Ca and K impurities were also detected in the film.

Optical transmittance measurements of ZTO films with different deposition temperature in the range of RT to 400 °C is shown in Fig. 3(a). The ZTO film exhibits higher transmission in the short wavelength region may analogous to increase in crystallite size. The average transmittance is above 85% secured by all the films in the visible wavelength region showing excellent optical property which is essential for using material as ETM in planer PSC or as a buffer layer in thin film solar cells. The optical bandgap (Eg) of the films can be determined from the absorption data using the Tauc relation as follows [41]:

$$(\alpha h\nu) = A(h\nu - Eg)^m \quad (4)$$

where α is the absorption coefficient, A is a constant, hν is the photon energy, Eg is the material's optical bandgap. The exponent 'm' depends on the type of transition and it may have values 1/2, 2, 3/2 and 3 corresponding to the allowed direct, allowed indirect, forbidden direct and forbidden indirect transitions, respectively. Since ZTO is direct bandgap material, thus m = 1/2 has been considered for the bandgap extrapolation. Fig. 3(c) shows the experimentally observed values of $(\alpha h\nu)^2$ plotted against hν enabling the energy bandgap to be determined. The variation of bandgap with the variation of substrate temperature is corresponding to the crystallographic variation of the films as seen in XRD spectra and SEM images. The lowest bandgap 3.65 eV has found for 300 °C of substrate temperature and highest 3.74 eV for RT. It has been reported that the band gap of Zn-Sn-O based semiconductors are ranging from 3.35 to 4.1 eV [42].

The average grain size in SEM images has been calculated using ImageJ software [43] and found that the average grain sizes are increased from 1.02 nm to 7.5 nm with the increase of substrate temperature from RT to 400 °C. Fig. 3(d) shows the relation between the grain size and bandgap of ZTO thin films prepared by different substrate temperature. It is well known that the bandgap of the thin films is reduced with the increase of grain sizes of the films. In this study also find a similar trend for all other films except the film prepared at 400 °C of substrate temperature. In this case, we think that the elemental composition played an important role in the effect of grain size.

The electronic properties of ZTO thin films were studied by Hall effects measurement. It is well known to that carrier mobility and carrier concentration are two key factors controlling the transport properties of traditional inorganic semiconductors. In particular, an ETM or buffer layer with high mobility and high carrier concentration are indispensable for using in PSC or heterojunction thin film solar cells. In this study, the electron concentrations were found in the range from 1.2×10^{16} to 2.5×10^{17} cm^{-3} depending upon substrate temperature and the O and Sn concentration of the film. Similar behavior has also been reported in sputtered a-ZTO thin films [38]. The simultaneous increase of mobility and carrier concentration as seen in Fig. 4 until the substrate temperature 300 °C may be related to the increase of Sn concentration and/or reduces of O concentration. Zhang et al. reported that the self-doping defect of Sn on Cd site forms shallow donor with low formation energy in the inverse spinel structure of $CdSnO_v$ (CTO) [44]. This defect is formed under oxygen deficient and Sn-rich, or equivalent conditions. Although, it is questionable regarding the sufficient similarities between the CTO and the ZTO thin film for apply CTO results to ZTO, however certainly Sn on Zn site self-doping defect as the source of carriers in ZTO seems prudent as observed the Sn/((Zn + Sn) ratios in Fig. 4. Besides, the highest carrier concentration of 2.5×10^{17} cm^{-3} is observed for materials grown at substrate temperatures of 300 °C and Sn/(Zn + Sn) ratio equal to 0.52. The change in electron concentration attributable to change in the native donor concentration into the ZTO lattice. It has been reported that the relatively high resistivity and/or low carrier concentration are related to the enhancement of oxygen concentration in the films and/or to oxygen adsorption on grain-boundary surfaces and carrier conduction is dominated by grain boundary scattering [45]. In general, the presence of oxygen vacancies in the oxide lattice leads to an increase in carrier concentration. The oxygen vacancies contribute two electrons to the electrical conduction since it could act as a double ionized donor as shown in the reaction:

$$O_0 \rightarrow V_o'' + 2e' + \frac{1}{2}O_2(g) \quad (1)$$

Thus, the carrier concentration in ZTO films could be controlled by oxygen-vacancy formation via annealing under a reducing atmosphere [46], however, charge carriers generated by oxygen reduction via thermal annealing are sensitive to process conditions making difficult to precisely control their concentrations. Alternatively, charge carriers could also increase by the Sn concentration, because Sn has two more valence electrons than Zn, and Sn acts as a donor by either occupying the interstitial sites or substituting for the Zn atom [46]. Besides, it is quite possible that grain boundary scattering may play a greater role

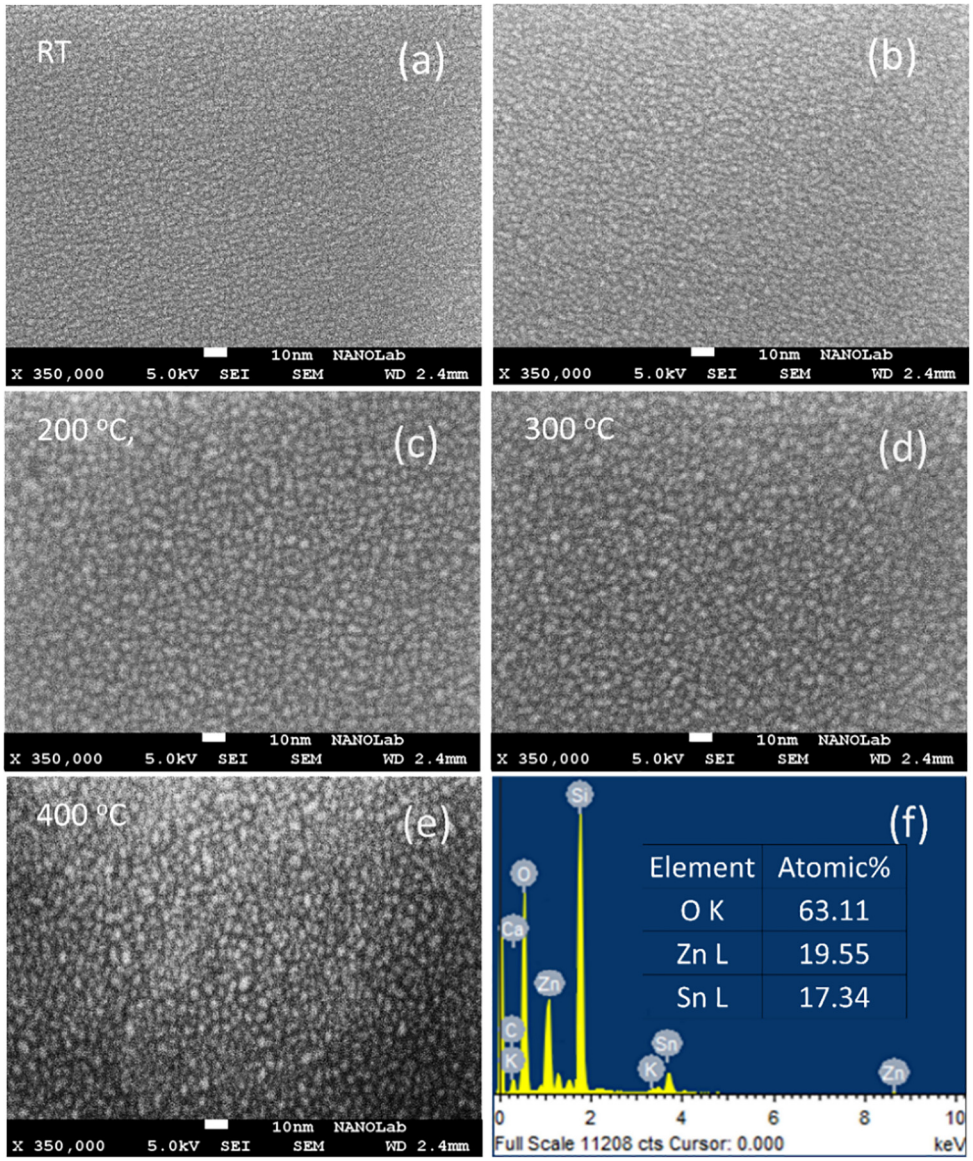

Fig. 2. (a)–(d) SEM surface morphology of the ZTO thin films prepared with different substrate temperature, and (f) EDX spectra of ZTO thin films prepared at 300 °C (inset shows the elemental composition of the film).

than is likely in a higher concentration of Sn material. For confirming the effect of ionized impurity defect, the carrier concentration versus mobility curve has been drawn as shown in Fig. 4(inset). The curve indicates that with the increase of substrate temperature towards 300 °C reduces the ionized impurity defects, leading to the improvement of carrier mobility. It is also indicated that the sub-bandgap defect in the ZTO films is reduced with the increase of substrate temperature. However, further increase of substrate temperature to 400 °C, mobility and carrier concentration both reduces implies that the increase of ionized defect density and sub-bandgap defect density at this temperature [47]. This may occur due to the increased grain boundary scattering via adsorption of excess O content in the film on grain boundary.

In this study, mobility has found to be in the range of 3.9–14.5 cm^2/Vs and the highest mobility is achieved for 300 °C of substrate temperature. The film mobility found in this study is quite high considering the films are amorphous in nature and although films were no longer annealed in the O free ambient to reduce the O content in the film. The high mobility might be due to low RF power as well as a relatively high argon pressure (8–10 mTorr) which was chosen for ZTO film deposition. These factors reduced the energy of the atoms in the chamber by increasing the number of collisions between gas molecules and thus minimize their damaging bombardment on the grown ZTO layer. Similar phenomena have also been discussed for ZnO thin films and reported in [48]. Higher stress, in particular, may increase the number of defects in the deposited layer, with a negative effect on carrier transport and mobility. The highest resistivity 30 Ω cm found for the film prepared at RT(27 °C) and the lowest resistivity 2.1 Ω cm found for the film of substrate temperature 300 °C. This drastic change of resistivity is unknown but may be related to the O and Sn concentration in the film as seen in Fig. 4. From the above analysis, it is clear that the film deposition temperature plays an important role in carrier concentration, mobility, and resistivity as well as elemental composition.

The perovskite solar cell (PSC) device performance utilizing ZTO as an electron transport material (ETM) has been conducted using the one-dimensional software SCAPS-1D (version 3.3.01). The thickness of the ZTO layer has been considered 100 nm and optoelectronic properties has been employed as we found this study. For details of SCAPS-1D including other layer parameters, readers are referred to the literature [49,50]. The PSC structure used for modeling including energy band diagram is shown in Fig. 5(a). Particularly, the most efficient PSCs to

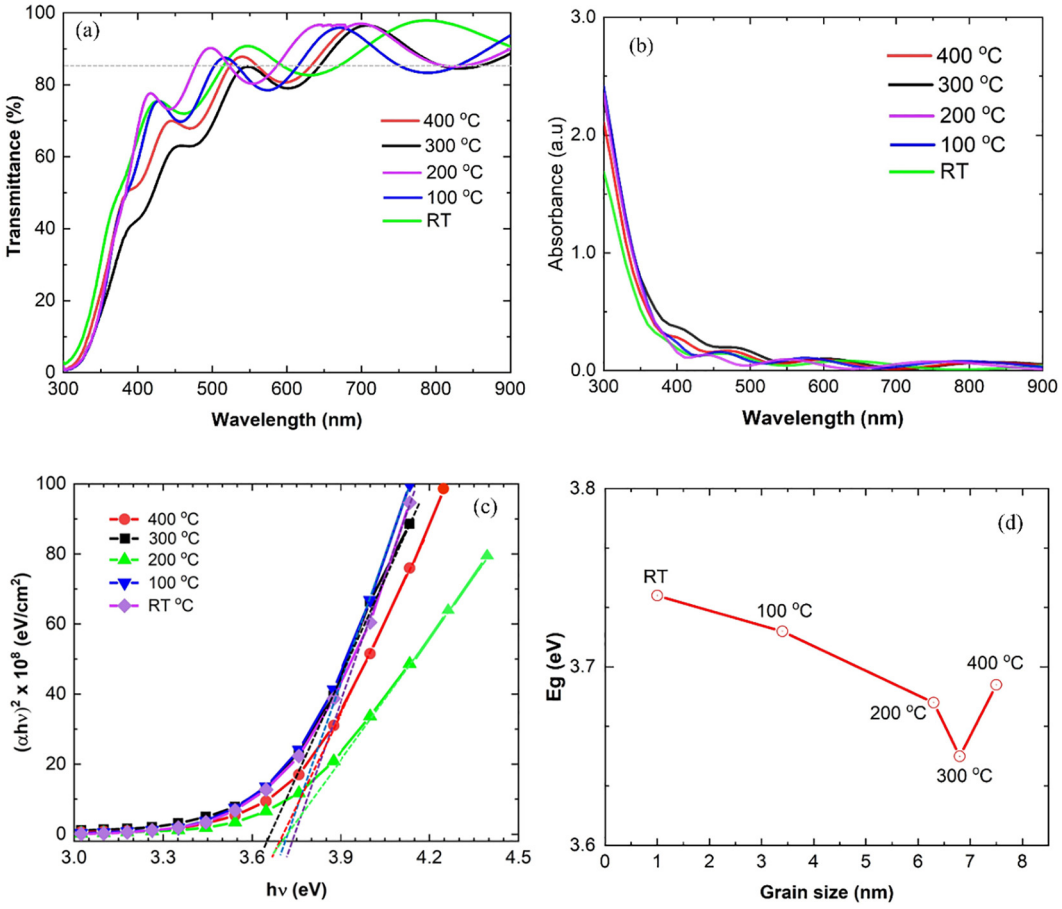

Fig. 3. (a) Transmittance spectra, (b) absorption spectra, (c) Tauc plot and (d) the relationship between grain size and the bandgap of ZTO thin films prepared by different substrate temperature.

date are having TiO_2 and/or ZnO based materials as ETM [51], however, as mentioned above, these ETM materials are found to inferior in overall performance in comparison efficiency, recombination mechanism, and stability. This drawback broadens the scope of developing new ETM materials for improving the efficiency and stability of PSC's. The superior properties of ZTO thin films have also been discussed in the earlier section. The only shortcoming of ZTO/perovskite PSCs is still low efficiency of 13.34% [28], which may be due to the presence of

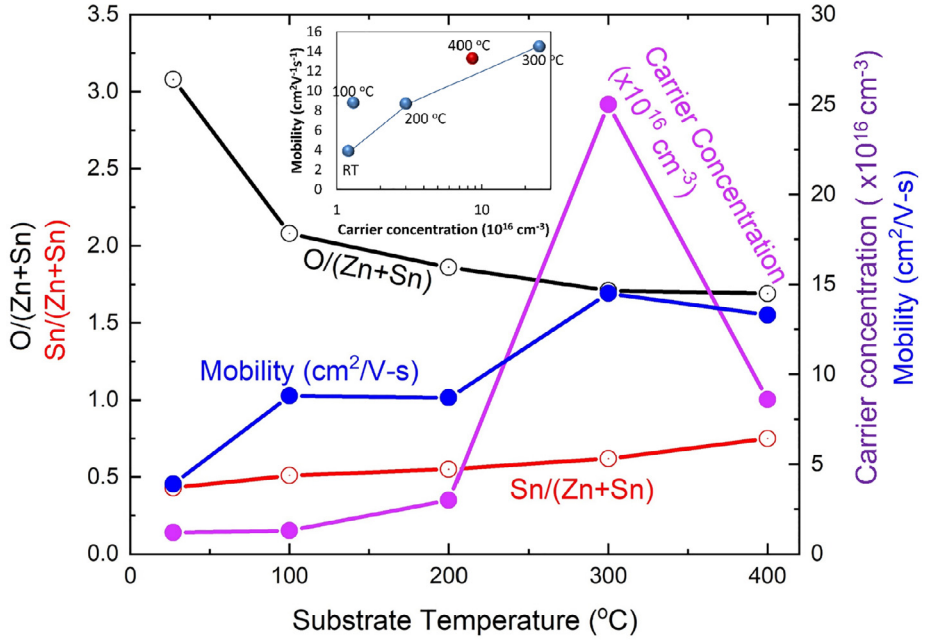

Fig. 4. Elemental composition, carrier concentration and mobility of ZTO thin films with respect to their substrate temperature.

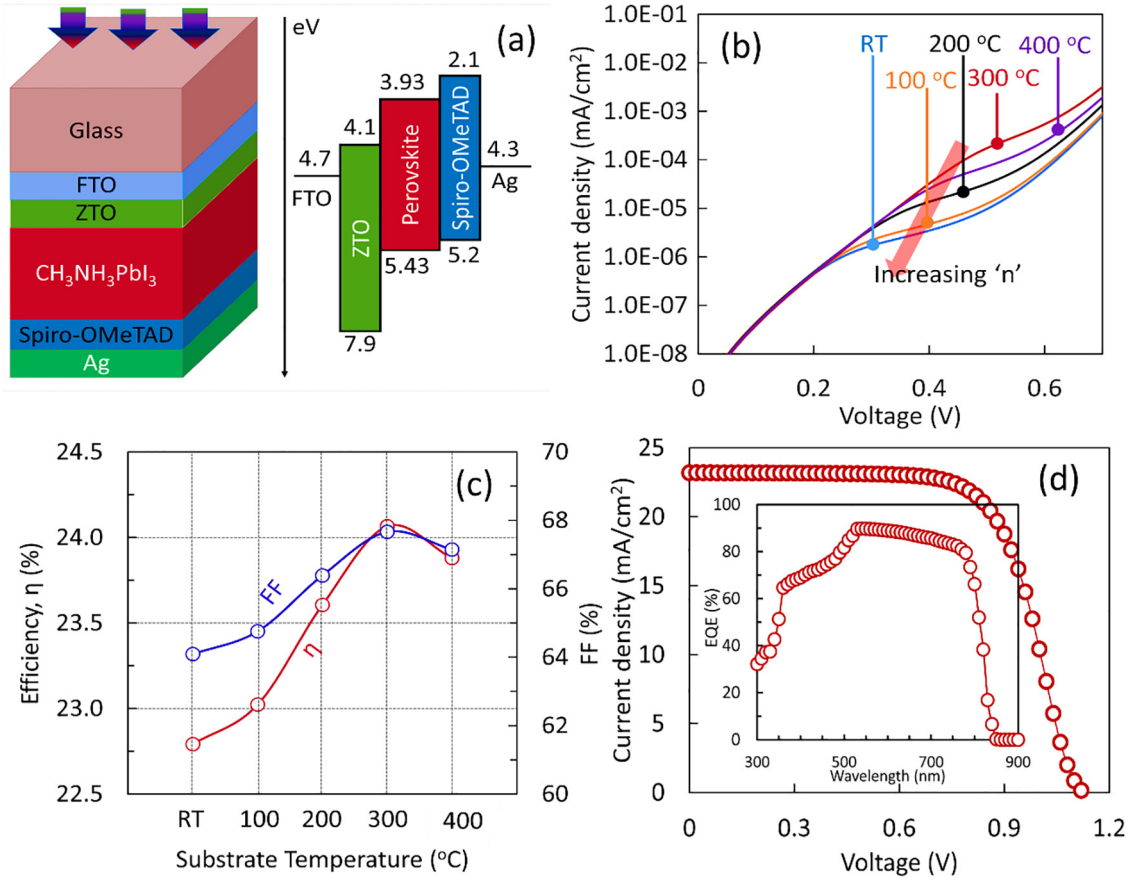

Fig. 5. (a) The structure of PSC and energy band diagram, (b) Semi-log plot of dark current–voltage (I–V) curve found for PSCs with different ZTO thin films deposited by different substrate temperature, (c) the variation of efficiency and fill factor with respect to the ZTO thin films deposited by different substrate temperature, and (d) the current density–voltage (J–V) curves of highest achieved conversion efficiency (24.07%) found for ZTO thin film of substrate temperature 300 °C (inset: quantum efficiency curve for the corresponding PSC).

interfacial defects, demanding much more study on ZTO/perovskite PSCs. It should be noticed that ZTO/perovskite is very less studied yet to date comparative to the TiO_2/perovskite, ZnO/perovskite, and SnO_2/perovskite although it is using widely in the other technologies. Fig. 5 show the results found from the numerical simulation utilizing the PSC structure of Glass/FTO/ZTO/$MAIPbI_3$/Spiro-OMeTAD/Ag.

Fig. 5(b) shows the semi-log plot of dark IV of the PSCs with different ZTO thin films as mentioned above. It could be observed that the lowest ideality factor and recombination current is for the film deposited by 300 °C. As the ZTO film of 300 °C substrate temperature secured the highest electron mobility and carrier concentration that may influence to reduce the ideality factor and dark recombination current. Fig. 5(c) shows the efficiency and FF variation with respect to ZTO film's deposition temperature. It has also been seen that Voc and Jsc are varied similar to FF although the variation is not significant (not shown here) for them. It is well known that FF is directly related to charge extraction and transport occurred in PSC. The charge extraction and transport depend on the carrier mobility, film morphology, and interfacial and bulk charge-recombination rates in the device. Also, the conventional p–i–n semiconductor models tell that the Jsc is determined by the spectral response of the light harvester and carrier recombination in the device, and the Voc depends on the splitting of the electron and hole quasi-Fermi energy levels in the whole device, [52] so it is affected by the energy distribution of the perovskite thin films and charge transport layer [53]. Fig. 5(d) and 5(d-inset) shows the IV curves and EQE for the highest achieved efficiency for ZTO prepared by 300 °C. The best efficiency achieved in this study is 24.07% with Voc of 1.13 eV, Jsc of 23.18 and fill factor (FF) of 67.66%. It is clearly seen that the properties ZTO thin films are affected significantly PSC's FF and efficiency indicate that much more study is demanding on ZTO ETM to get the highest efficiency and stable PSCs. From this study, it is also found that the ZTO could be more potential ETM than conventionally using nowadays in PSCs.

Conclusion

We have demonstrated the properties of ZTO films of thickness around 100 nm prepared by reactive co-sputtering technique. The uniform microstructure with compact interconnected grains was seen in SEM images and these grains are covered the substrate surface homogeneously. The film transmission is higher than 85% in the visible region and substrate temperature had seemed a significant effect on the optical properties. The bandgap was observed to reduce with the increase of grain size. The carrier mobility is as high as 14.5 cm^2/Vs measured by Hall-Effect measurement which is quite high with respect to the amorphous film structure independent of the applied deposition process. It was found that the substrate temperature playing an important role in the film's electrical properties. The resistivity of the films found in the range of 2.1–30 Ω cm, which is limited by the low carrier concentration in the range of 1.2–25 × 10^{16} cm^{-3} rather than by the mobility. The experimentally found lector-optical properties have been employed for numerically modeling of PSC using SCAPS-1D. It has been found that the film electrical properties such as mobility and carrier concentration significantly affect the device ideality factor, recombination current which ultimately affects the device conversion efficiency. The highest efficiency achieved in this study is 24.07% with Voc of 1.13 eV, Jsc of 23.18 and fill factor (FF) of 67.66%. The numerical simulation results indicate that ZTO could be very ETM for

stable and high-efficiency PSCs.

Acknowledgment

The authors would like to acknowledge and appreciate the contribution of the Institute of Sustainable Energy (ISE) of the Universiti Tenaga Nasional (@The National Energy University) of Malaysia for their support through BOLD2025 Program. Due appreciation is also credited to The Solar Energy Research Institute of The National University of Malaysia (@UKM) for other supports.

Appendix A. Supplementary material

Supplementary data to this article can be found online at https://doi.org/10.1016/j.rinp.2019.102518.

References

[1] Kim HS, Lee CR, Im JH, Lee KB, Moehl T, Marchioro A, et al. Lead iodide perovskite sensitized all-solid-state submicron thin film mesoscopic solar cell with efficiency exceeding 9%. Sci Rep 2012;2:591.
[2] Lee MM, Teuscher J, Miyasaka T, Murakami TN, Snaith HJ. Efficient hybrid solar cells based on meso-superstructured organometal halide perovskites. Science 2012;6107:643–7.
[3] Krishnan U, Kaur M, Kumar M, Kumar A. Factors affecting the stability of perovskite solar cells: a comprehensive review. J Photon Energy 2019;9(2):021001.
[4] Baikie T, Fang Y, Kadro JM, Schreyer M, Wei F, Mhaisalkar SG, et al. Synthesis and crystal chemistry of the hybrid perovskite (CH3NH3)PbI3 for solid-state sensitised solar cell applications. J Mater Chem A 2013;1(18):5628–41.
[5] Meng Y, Lan C, Li F, Yip S, Wei R, Kang X, et al. Direct vapor-liquid-solid synthesis of all-inorganic perovskite nanowires for high-performance electronics and optoelectronics. ACS Nano 2019.
[6] Wehrenfennig C, Eperon GE, Johnston MB, Snaith HJ, Herz LM. High charge carrier mobilities and lifetimes in organolead trihalide perovskites. Adv Mater 2014;26(10):1584–9.
[7] Alamri AM, Leung S, Vaseem M, Shamim A, He JH. Fully inkjet-printed photodetector using a graphene/perovskite/graphene heterostructure. IEEE Trans Electron Dev 2019;66(6):2657–61.
[8] Poindexter JR, Hoye RL, Nienhaus L, Kurchin RC, Morishige AE, Looney EE, et al. High tolerance to iron contamination in lead halide perovskite solar cells. ACS Nano 2017;11(7):7101–9.
[9] Ouyang W, Teng F, He JH, Fang X. Enhancing the photoelectric performance of photodetectors based on metal oxide semiconductors by charge-carrier engineering. Adv Funct Mater 2019;29(9):1807672.
[10] Yang W, Hu K, Teng F, Weng J, Zhang Y, Fang X. High-performance silicon-compatible large-area UV-to-visible broadband photodetector based on integrated lattice-matched type II Se/n-Si heterojunctions. Nano Lett 2018;18(8):4697–703.
[11] Jin H, Li J, Iocozzia J, Zeng X, Wei PC, Yang C, et al. Hybrid organic-inorganic thermoelectric materials and devices. Angew Chem 2019.
[12] Berhe TA, Su WN, Chen CH, Pan CJ, Cheng JH, Chen HM, et al. Organometal halide perovskite solar cells: degradation and stability. Energy Environ Sci 2016;9(2):323–56.
[13] Yang WS, Park BW, Jung EH, Jeon NJ, Kim YC, Lee DU, et al. Iodide management in formamidinium-lead-halide–based perovskite layers for efficient solar cells. Science 2017;356(6345):1376–9.
[14] Yu L, Luo D, Wang H, Zou T, Luo L, Qiao Z, et al. Highly conductive Zinc-Tin-Oxide buffer layer for inverted polymer solar cells. Org Electron 2016;33:156–63.
[15] Alpuche-Aviles MA, Wu Y. Photoelectrochemical study of the band structure of Zn2SnO4 prepared by the hydrothermal method. J Am Chem Soc 2009;131(9):3216–24.
[16] Shin SS, Yang WS, Noh JH, Suk JH, Jeon NJ, Park JH, et al. High-performance flexible perovskite solar cells exploiting Zn2 SnO4 prepared in solution below 100 C. Nat Commun 2015;6:7410.
[17] Yang WS, Noh JH, Jeon NJ, Kim YC, Ryu S, Seo J, et al. High-performance photovoltaic perovskite layers fabricated through intramolecular exchange. Science 2015;348(6240):1234–7.
[18] Liu H, Huang Z, Wei S, Zheng L, Xiao L, Gong Q. Nano-structured electron transporting materials for perovskite solar cells. Nanoscale 2016;8(12):6209–21.
[19] Leijtens T, Eperon GE, Pathak S, Abate A, Lee MM, Snaith HJ. Overcoming ultraviolet light instability of sensitized TiO2 with meso-superstructured organometal tri-halide perovskite solar cells. Nat Commun 2013;4:2885.
[20] Fang R, Zhang W, Zhang S, Chen W. The rising star in photovoltaics-perovskite solar cells: the past, present and future. Sci China Technol Sci 2016;59(7):989–1006.
[21] Zhang Y, Xu W, Xu X, Cai J, Yang W, Fang X. Self-powered dual-color UV-green photodetectors based on SnO2 millimeter wire and microwires/CsPbBr 3 particles heterojunctions. J Phys Chem Lett 2019.
[22] Roose B, Baena JP, Gödel KC, Graetzel M, Hagfeldt A, Steiner U, et al. Mesoporous SnO2 electron selective contact enables UV-stable perovskite solar cells. Nano Energy 2016;30:517–22.
[23] Ke W, Fang G, Liu Q, Xiong L, Qin P, Tao H, et al. Low-temperature solution-processed tin oxide as an alternative electron transporting layer for efficient perovskite solar cells. J Am Chem Soc 2015;137(21):6730–3.
[24] Mahmood K, Swain BS, Amassian A. 16.1% Efficient hysteresis-free mesostructured perovskite solar cells based on synergistically improved ZnO nanorod arrays. Adv Energy Mater 2015;5(17):1500568.
[25] Tong SW, Balapanuru J, Fu D, Loh KP. Thermally stable mesoporous perovskite solar cells incorporating low-temperature processed graphene/polymer electron transporting layer. ACS Appl Mater Interfaces 2016;8(43):29496–503.
[26] Yang J, Siempelkamp BD, Mosconi E, De Angelis F, Kelly TL. Origin of the thermal instability in CH3NH3PbI3 thin films deposited on ZnO. Chem Mater 2015;27(12):4229–36.
[27] Lian J, Lu B, Niu F, Zeng P, Zhan X. Electron-transport materials in perovskite solar cells. Small Methods 2018;2(10):1800082.
[28] Bera A, Sheikh AD, Haque MA, Bose R, Alarousu E, Mohammed OF, et al. Fast crystallization and improved stability of perovskite solar cells with Zn2SnO4 electron transporting layer: interface matters. ACS Appl Mater Interfaces 2015;7(51):28404–11.
[29] Liu X, Chueh CC, Zhu Z, Jo SB, Sun Y, Jen AK. Highly crystalline Zn2SnO4 nanoparticles as efficient electron-transporting layers toward stable inverted and flexible conventional perovskite solar cells. J Mater Chem A 2016;4(40):15294–301.
[30] Lana-Villarreal T, Boschloo G, Hagfeldt A. Nanostructured zinc stannate as semiconductor working electrodes for dye-sensitized solar cells. J Phys Chem C 2007;111(14):5549–56.
[31] Oo TZ, Chandra RD, Yantara N, Prabhakar RR, Wong LH, Mathews N, et al. Zinc Tin Oxide (ZTO) electron transporting buffer layer in inverted organic solar cell. Org Electron 2012;13(5):870–4.
[32] Ferekides CS, Mamazza R, Balasubramanian U, Morel DL. Transparent conductors and buffer layers for CdTe solar cells. Thin Solid Films 2005;480:224–9.
[33] Islam MA, Rahman KS, Sobayel K, Enam T, Ali AM, Zaman M, et al. Fabrication of high efficiency sputtered CdS: O/CdTe thin film solar cells from window/absorber layer growth optimization in magnetron sputtering. Sol Energy Mater Sol Cells 2017;172:384–93.
[34] Takamoto T, Agui T, Kurita H, Ohmori M. Improved junction formation procedure for low temperature deposited CdS/CdTe solar cells. Sol Energy Mater Sol Cells 1997;49(1–4):219–25.
[35] Minami T, Nishi Y, Miyata T. Effect of the thin Ga2O3 layer in n+-ZnO/n-Ga2O3/p-Cu2O heterojunction solar cells. Thin Solid Films 2013;549:65–9.
[36] Chiang HQ, Wager JF, Hoffman RL, Jeong J, Keszler DA. High mobility transparent thin-film transistors with amorphous zinc tin oxide channel layer. Appl Phys Lett 2005;86(1):013503.
[37] Patil MA, Mujawar SH, Ganbavle VV, Rajpure KY, Deshmukh HP. Synthesis and characterization of zinc stannate thin films prepared by spray pyrolysis technique. J Mater Sci: Mater Electron 2016;27(12):12323–8.
[38] Rajachidambaram JS, Sanghavi S, Nachimuthu P, Shutthanandan V, Varga T, Flynn B, et al. Characterization of amorphous zinc tin oxide semiconductors. J Mater Res 2012;27(17):2309–17.
[39] Kim DH, Cho NG, Kim HG, Choi WY. Structural and electrical properties of indium doped ZnO thin films fabricated by RF magnetron sputtering. J Electrochem Soc 2007;154(11):H939–43.
[40] Caruge JM, Halpert JE, Wood V, Bulović V, Bawendi MG. Colloidal quantum-dot light-emitting diodes with metal-oxide charge transport layers. Nat Photon 2008;2(4):247.
[41] Islam MA, Hossain MS, Aliyu MM, Karim MR, Razykov T, Sopian K, et al. Effect of $CdCl_2$ treatment on structural and electronic property of CdTe thin films deposited by magnetron sputtering. Thin Solid Films 2013;546:367–74.
[42] Satoh K, Kakehi Y, Okamoto A, Murakami S, Uratani F, Yotsuya T. Influence of oxygen flow ratio on properties of Zn2SnO4 thin films deposited by RF magnetron sputtering. Jpn J Appl Phys 2004;44(1L):L34.
[43] Islam MA, Khandaker MU, Amin N. Effect of deposition power in fabrication of highly efficient CdS: O/CdTe thin film solar cell by the magnetron sputtering technique. Mater Sci Semicond Process 2015;40:90–8.
[44] Zhang SB, Wei SH, Zunger A. Intrinsic n-type versus p-type doping asymmetry and the defect physics of ZnO. Phys Rev B 2001;63(7):075205.
[45] Minami T, Nanto H, Takata S. Highly conductive and transparent zinc oxide films prepared by rf magnetron sputtering under an applied external magnetic field. Appl Phys Lett 1982;41(10):958–60.
[46] Jeong S, Jeong Y, Moon J. Solution-processed zinc tin oxide semiconductor for thin-film transistors. J Phys Chem C 2008;112(30):11082–5.
[47] Rucavado E, Jeangros Q, Urban DF, Holovský J, Remes Z, Duchamp M, et al. Enhancing the optoelectronic properties of amorphous zinc tin oxide by subgap defect passivation: a theoretical and experimental demonstration. Phys Rev B 2017;95(24):245204.
[48] Carcia PF, McLean RS, Reilly MH, Nunes Jr G. Transparent ZnO thin-film transistor fabricated by rf magnetron sputtering. Appl Phys Lett 2003;82(7):1117–9.
[49] Toshniwal A, Jariwala A, Kheraj V, Opanasyuk AS, Panchal CJ. Numerical simulation of tin based perovskite solar cell: effects of absorber parameters and hole transport materials. J Nano- Electron Phys 2017;9(3).
[50] Du HJ, Wang WC, Gu YF. Simulation design of P-I–N-type all-perovskite solar cells with high efficiency. Chin Phys B 2017;26(2):028803.
[51] Liu D, Kelly TL. Perovskite solar cells with a planar heterojunction structure prepared using room-temperature solution processing techniques. Nat Photon 2014;8(2):133.
[52] Edri E, Kirmayer S, Henning A, Mukhopadhyay S, Gartsman K, Rosenwaks Y, et al. Why lead methylammonium tri-iodide perovskite-based solar cells require a mesoporous electron transporting scaffold (but not necessarily a hole conductor). Nano Lett 2014;14(2):1000–4.
[53] Shao Y, Yuan Y, Huang J. Correlation of energy disorder and open-circuit voltage in hybrid perovskite solar cells. Nat Energy 2016;1(1):15001.